Study of 2D Graphene topological properties

Antonio Lacerda ; Florie Mesple
Université Grenoble Alpes
(Dated: december 2017)

Here we present a numerical study of the 2D graphene density of states and energy dispersion. They were calculated using two different methods. The first is a purely numerical approach, where the 2D graphene lattice and its first and second neighbours connections were obtained with a python script and used to obtain the Hamiltonian of the system according to the Haldane model. The second approach is purely analytical and a python script was used to calculated the density of states and energy dispersion using the deduced equations. Finally, the chern number of the 2D graphene was obtained from the numerical approach.

I. INTRODUCTION

Monolayer graphene, with its simple but property rich honeycomb lattice, has attracted a lot of attention from a theoretical perspective. Moreover, since its demonstration by Nosolov et al.[8] in 2004 a surge in the efforts to understand its properties as well as to apply them to make new and rather unexpected devices took place [4]. From a condensate matter theory point of view, the honeycomb lattice allows for many intriguing properties, such as massless Dirac fermions (near the Dirac cone) [7], anomalous quantum hall effect, fractional hall effect and topologically protected states [1]. Concerning the latter, the next-nearest-neighbour interactions in the honeycomb lattice allows for topological insulator properties to appear in the monolayer graphene. More precisely, the berry phase gained by an electron when tunnelling from an atomic position to the other within the same graphene sub-lattice allow for a gap opening in the graphene band dispersion, which makes the latter a Chern-insulator, a sub-group of topological insulators. Indeed, for Chern insulators, not only there are conducting edge states (in contrast to the insulating bulk), but time-reversal symmetry is also broken [2]. This, as hinted earlier, is due to the imaginary phase acquired when electrons hop from an atom to the other within the same graphene sublattice. Graphene was predicted to be a Chern insulator by using the Haldane model [5]. In fact, using the latter one can calculate the monolayer graphene density of states, and then use the latter to deduce its chern number. If the latter is non-trivial, i.e. $\neq 0$, and equal to ± 1, one has demonstrated monolayer graphene to be a Chern-insulator. In the remaining of this article the graphene DOS will be analytically (Sec.II B) and numerically (Sec.II C) calculated using the Haldane model mentioned before. Later the Chern number will be calculated using the method proposed by Fukui et al [3].

II. GRAPHENE LATTICE, HAMILTONIAN AND DENSITY OF STATES

A. The Honycomb Lattice

The graphene honeycomb lattice is shown in Fig.1a. There exists two inequivalent sublattices named A and B. To each sublattice one can associate a Bravais lattice with primitive lattice vectors :

$$\vec{a_1} = \frac{a}{2}(3, \sqrt{3}) \quad \text{AND} \quad \vec{a_2} = \frac{a}{2}(3, -\sqrt{3}) \tag{1}$$

where a is the inter-atomic distance. From Eq.1 one can deduce the following reciprocal lattice vectors :

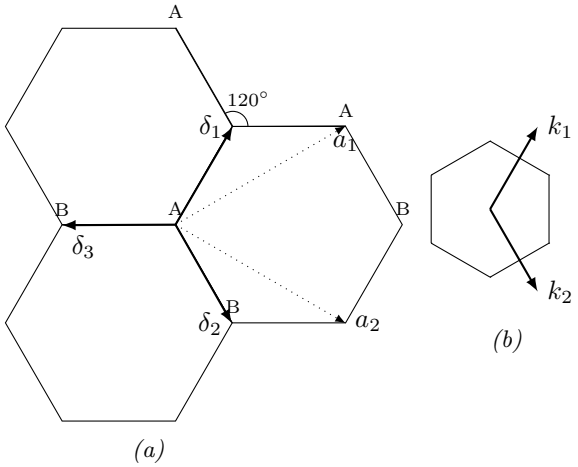

Figure 1: a) shows the honeycomb lattice with two sub-lattices definition and associated vectors and b) shows the graphene Brillouin zone and associated vectors.

$$\vec{k_1} = \frac{2\pi}{3a}(1, \sqrt{3}) \quad \text{AND} \quad \vec{k_2} = \frac{2\pi}{3a}(1, -\sqrt{3}) \tag{2}$$

And the Brillouin zone can be seen in Fig.1b.

In the sublattice A the vector defining the three nearest neighbours are :

$$\delta_1 = \frac{a}{2}(1, \sqrt{3}) \quad ; \quad \delta_2 = \frac{a}{2}(1, -\sqrt{3}) \quad ; \quad \delta_3 = -a(1, 0) \tag{3}$$

Whereas for the sublattice B they are the negative of those defined in Eq.3.

B. Analytical Calculations

The full Hamiltonian proposed by Haldane [5] in order to model the honeycomb lattice (neglecting here an average lattice potential V) is the following :

$$H = \sum_i (-1)^i M \left|i\right\rangle \left\langle j\right| - \sum_{\langle ij \rangle} t_1 \left|i\right\rangle \left\langle j\right| - \sum_{\langle\langle ii^* \rangle\rangle} t_2 e^{i\phi_{ii^*}} \left|i\right\rangle \left\langle i^*\right| + \text{h.c} \tag{4}$$

where M is the difference in potential energy between the A and B sites, i.e. between a site i and its nearest neighbour j, which is set to 0 throughout this work. The second term

corresponds to the nearest neighbour hopping, with t_1 as the transfer constant. The third term corresponds to the next-nearest neighbour hopping, with t_2 as the transfer term and ϕ_{ii^*} the so called berry phase gained by the electron. Here h.c corresponds to the hermitian conjugate, $|i\rangle$ and $\langle j|$ respectively stand for the creation and annihilation of a given state, thus represent the hopping from one site to its nearest neighbour. Concerning $\langle i^*|$, it is defined in the same way as $\langle j|$ but for the next-nearest neighbour.

One can write :

$$\begin{aligned} |i\rangle &= \tfrac{1}{\sqrt{N}} \sum k e^{-i\vec{k}\vec{r_i}} |k\rangle \\ \langle j| &= \tfrac{1}{\sqrt{N}} \sum k' e^{i\vec{k'}\vec{r_j}} \langle k'| \end{aligned} \tag{5}$$

Where $\vec{k}$ and $\vec{k'}$ correspond to the momentum point in the reciprocal space and r the coordinates of the corresponding site. One can thus write :

$$\begin{aligned} H = -\frac{1}{N}\Bigg[&\sum_k \sum_{k'} \sum_{\langle ij \rangle} t_1 e^{-i(k-k')r_i} e^{ik'au_x} |k\rangle \langle k'| \\ &- \sum_k \sum_{\langle ii^* \rangle} t_2 e^{i\phi_{ii^*}} e^{iku^*_{xi^*}} |k\rangle \langle k| \\ &- \sum_{k'} \sum_{\langle jj^* \rangle} t_2 e^{i\phi_{jj^*}} e^{ik'u^*_{xj^*}} |k'\rangle \langle k'| + \text{h.c} \Bigg] \end{aligned} \tag{6}$$

where $r_j - r_i = au_x$, $r_{i^*,j^*} - r_{i,j} = u^*_{xj^*,xi^*}$, with i^* and j^* the next-nearest neighbour of i and j respectively (here i and j corresponds to the atoms in the A and B sublattices respectively). Moreover, since $e^{-i(k-k')r_i} = \delta(k-k')$ one can thus write $\sum_k e^{i(k-k')r_i} = 1$. In addition, by using the vectors defined in Eq.3 to describe the distance between a site and its 3 nearest neighbours and its 6 next-nearest neighbours, one can write :

$$\begin{aligned} H = -\frac{1}{N}\Bigg[&t_1 \sum_k \sum_{l=1}^{3} e^{ik'\delta l} |k\rangle \langle k'| \\ &- t_2 \sum_{l=1}^{6} e^{i\phi_l} \left(\sum_k e^{ik\delta_l^*} |k\rangle \langle k| + \sum_{k'} e^{-ik'\delta_l^*} |k'\rangle \langle k'| \right) + \text{h.c} \Bigg] \end{aligned} \tag{7}$$

with δ_l the vectors describing the hopping between the nearest-neighbours and shown in Eq.3, δ_l^* a linear combination of the vectors in Eq.3 describing the next-nearest neighbour hopping [**Note1**] and $\phi_l = (-1)^{l+1}\pi/2$. Therefore, one can can define define H_0 as the first term in Eq.7 (next to t_1) and H_{soc} as the second term (containing the berry phase ϕ_l) so that for each k;k' :

$$H = H_0 + H_{soc} + \text{h.c} = \begin{bmatrix} H_{soc}(k) + h.c & H_0 \\ H_0^\dagger & H_{soc}(k') + h.c \end{bmatrix} \tag{8}$$

The one-electron Hamiltonian matrix, for a given k and in the first-neighbour approach, yields a purely off-diagonal 2x2 Hamiltonian (Eq.8, with $H_{soc} = 0$). The latter can be diagonalised to yield the eigenvalues. It can be noted that being "off-diagonal" reflects the "A to B" and "B to A" sub-lattices hopping of the considered eletron. By applying this for every possible k, i.e. for every possible atomic position in the lattice, one obtains the eigenvalues of the whole system.Then, $\rho \cdot dE = dn$ can be used to find the DOS. The obtained result for $t_1 = 1$ is shown in Fig.2. One can see the expected "cone" shaped DOS near $E = 0$, which reflects the Dirac cone in the band dispersion and is in agreement with the literature [1].

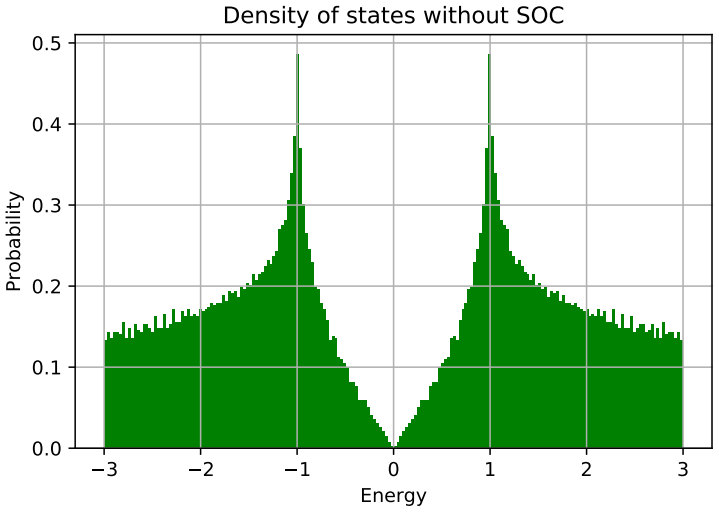

Figure 2: Density of States of graphene without Spin Orbit Coupling, obtained with the fourier transform method. The Dirac cone is clearly visible

If one takes into account the spin-orbit coupling, diagonal terms appear (as shown in Eq.8, with $H_{soc} \neq 0$) since they reflect "A to A" and "B to B" interactions. By setting $t_2 = 0.5$, $t_1 = 1$, the result obtained is shown in Fig.3a. One can see that, as expected, the coupling between two identical atoms, i.e. the non zero berry phase, induces a gap opening. One can thus see that the monolayer graphene will be an insulator. Moreover, Fig.3b shows that the gap increases linearly with the ratio t_2/t_1 and attains a maximum value equal to t_1 when the $t_2/t_1 = 0.1$.

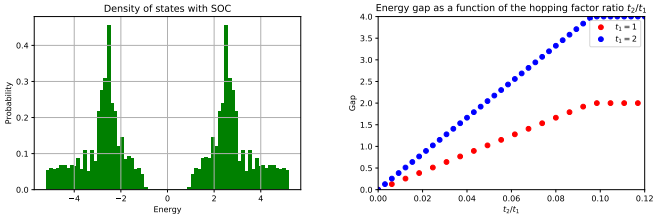

(a) *(b)*

Figure 3: a) shows the density of States of monoloayer graphene with Spin Orbit Coupling, obtained with the Fourier transform (analytically) method and b) shows the gap as a function of t_2/t_1 ratio. The later shows that the gap reaches its maximum value for $t_2/t_1 = 0.1$, which increases with t_1.

C. Numerical Calculations

The second approach used to calculate the graphene DOS is a purely numerical one. In the latter, a mesh with $n = n_x * n_y$

atoms occupying the atomic positions of the hexagonal lattice is constructed. In the latter the boundary condition is set so that a modulo operation is performed whenever the point in consideration has a neighbour outside of the mesh, e.g. the first atom has one of its neighbour the last atom in the mesh. The interaction of each atom in the mesh is then written so that a $n \times n$ matrix H representing the Haldane Hamiltonian of the system (see Eq.4) is constructed. In the latter, similarly to Sec.II B, its nearest neighbour interaction is represented by the term t_1 at the position ij, e.g. $H_{ij} = t_1$, with j corresponding to any of its three nearest neighbours, and its next-nearest neighbour interaction by a term t_2 at the position ii', e.g. $H_{ii'} = t_2$, with i' corresponding to any of its six next-nearest neighbours (t_2 changes sign depending on which next-nearest neighbour is being considered). The H matrix is then diagonalized so that its eigenvalues and eigenvectors, which correspond to, respectively, the energies and functions at each point in the reciprocal lattice of the system (in the new basis where H is diagonal), are obtained.

The DOS obtained for $t_1 = 1$, $t_2 = 0$ and $n = n_x = n_y = 54$ (the mesh size is $2n^2$) is shown in the first plot in Fig.4 and for $t_1 = 1$, $n = 54$ and $t_2 = 0.4j$ is shown in the second plot in Fig.4. Albeit a coarse mesh was used, the DOS for the $t_2 = 0$ case is in agreement with the one obtained analytically. Moreover, a gap is successfully open for $t_2 = 0.4$, which is expected from the analytical results. More importantly, the value for the energy gap obtained is not noticeably affected by the mesh size (for $n_x = n_y = 24$ it remains at 2) and matches the one obtained analytically (value of 2).

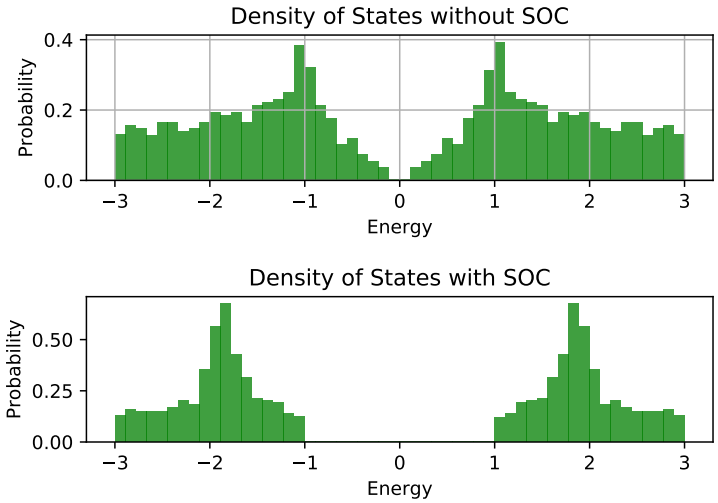

Figure 4: Density of States of graphene for different Hamiltonians : without Spin Orbit Coupling (upper histogram) ; with Spin Orbit Coupling (lower histogram).

III. CHERN NUMBERS IN THE HEXAGONAL LATTICE

The chern number is a topological quantum number that can be used to characterise the monolayer graphene and, (somewhat) more broadly, a solid with an hexagonal lattice [6]. More precisely, when a 2D solid has a non-vanishing chern number, it belongs to the group of chern insulators. These materials have (topologically protected) conduction bands on the edge and an insulating bulk. More interestingly, the difference between the number of edge states propagating "clockwise" and propagating "anti-clokwise" is equal to the chern number C_n, i.e. the net number of conducting edge states is equal to C_n [2]. Therefore, calculating such topological number can give insight on the electrical conduction of materials such as those described by a hexagonal lattice, e.g. monolayer graphene.

In the continuum case, the Chern number is given by the integral of the Berry curvature over the Brillouin zone (BZ) of the lattice [3] :

$$C_n = \frac{1}{2\pi i} \int_{BZ} d^2k F_{12}(k) \tag{9}$$

where $F_{12}(k) = \nabla_\mu \langle n(k)|\partial\mu|n(k)\rangle$ is the berry curvature, $|n(k)\rangle$ is a normalized Bloch wave function and the derivative $\partial 1, 2$ stands for $\frac{\partial}{\partial k_{1,2}}$, with $k_{1,2}$ the k vector defining the position of a site in the reciprocal lattice along the 2 different directions (not the reciprocal lattice vector as defined in Eq.2).

Since when doing numerical calculations the Brillouin zone is discretized (as it has been done in Sec.II B and Sec.II C), the continuum definition can no longer be used. One must thus calculate the chern number using the Berry flux, i.e. [2]:

$$C_n = \frac{1}{2\pi} \sum_{mn} F_{nm} \tag{10}$$

with F_{nm} the Berry flux, defined as :

$$F_{nm} = -arg\big[exp\big(\phi_{(n,m),(n+1,m)} + \phi_{(n+1,m),(n+1,m+1)} + \phi_{(n+1,m+1),(n,m+1)} + \phi_{(n,m+1),(n,m)}\big)\big] \tag{11}$$

where $\phi_{(n,m),(n+1,m)}$ correspond to the berry phase gained when an electron goes from the site (n, m) in the lattice to the site $(n, m + 1)$, and the sum is made over all closed contours defined within the reciprocal lattice of the solid [2]. Although it might seem straightforward to use Eq.10 to obtain the chern number numerically, when diagonalizing the Hamiltonian to obtain the eigenvectors one must be careful when evaluating the phase from the imaginary part of the eigenvectors. One method to reliably obtain a gauge invariant and interger chern number is to use the technique described by Fukui et al. [3].

In the latter, one divides the space into unit cells of size $\frac{2\pi}{(q_2 q_2 N_B)}$, with the BZ defined by $0 < k_{1,2} < 2\pi/q_{1,2}$ and $q_{1,2}$ integers. This can be done by assuming periodicity in the lattice : $|n(k_l)\rangle = |n(k_l + N_\mu \vec{\mu})\rangle$, with $\mu = \{1, 2\}$, $\|\vec{\mu}\| = \frac{2\pi}{q_\mu N\mu}$ and $N_\mu = q_\nu N_B$, $\nu \neq \mu$. This allows one to write the unit cell shown in Fig.5, with $\vec{1}$ and $\vec{2}$ the vectors defining the translation to, respectively, the left and above the initial point in the cell described by $\vec{k_l}$.

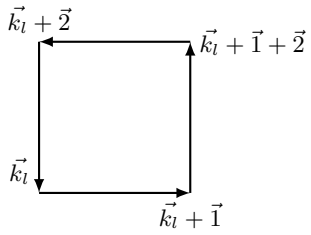

Figure 5: Unit cell and vectors defining circulation.

From Fig.5 and as demonstrated by Fukui et al.[3], one can define a normalised link variable as :

$$U_\mu(k_l) = \frac{\langle n(k_l)|n(k_l+\vec{\mu})\rangle}{\| \langle n(k_l)|n(k_l+\vec{\mu})\rangle \|} \tag{12}$$

The latter can be seen as the imaginary part of the eigenvector and, thus, the berry phase. From this, it is not surprising that a lattice berry flux (defined as a lattice field strength by Fukui et al[3]), can be written as :

$$\tilde{F}_{12} = ln(U_1(k_l)U_2(k_l+\vec{1})U_1(k_l+\vec{2})^{-1}U_2(k_l)^{-1}) \tag{13}$$

with $-\pi < \tilde{F}_{12}/i < \pi$. The chern number for the nth band can then be calculated as :

$$\tilde{c}_n = \frac{1}{2\pi i}\sum_l \tilde{F}_{12}(k_l) \tag{14}$$

Two important considerations must be made here : i) the chern number cannot be calculated if two bands touch or overlap and ii) the critical mesh size, for which the chern number obtained is reliable, is $N_B^c = \mathrm{O}\sqrt{2|c_n|(q_1q_2)}$, with q_1 and q_2 the same integers defined earlier [3].

The chern number was thus calculate using $Eq.14$ for a mesh of size $2n^2$, with $n = 54$, $t_1 = 1$ and $t_2 = 0.4j$ and using the eigenvectors obtained from the diagonalization of the matrix H defined in Sec.II C. The result obtained for the energy band bellow $E = 0$ is $\tilde{c}_n^- = -2.63$ and for the one above $E = 0$ is $\tilde{c}_n^+ = -3.527$. These results change very little with mesh size (for $n = 24$ the values $\tilde{c}_n^- = -2.34$ and $\tilde{c}_n^+ = -3.923$). However, from the condition mentioned in the previous paragraph they should not change as long as the mesh size is above N_c, with q_1 and q_2 being integers and c_n the chern number, which is expected to be ± 1 for the hexagonal lattice. Moreover, the chern numbers as integer values, contrary to what is obtained here. Therefore, the results presented in this work are not reliable.

Considering that the numerical results for the DOS seems to be in agreement with the analytical ones and to be independent of the mesh size for $n > 12$, the source of the error might be in the calculation of the chern number, i.e. in how we implemented the method described by Fukui et.al [3]. The reason(s) for the discrepancy between what was expected (Chern values of ± 1) and the numerical results is still unknown.

IV. CONCLUSION

In this work, the hexagonal lattice of graphene was studied. Two different methods have been used to calculate the graphene density of states. The analytical one showed a high degree of accuracy, which is expected. The results obtained with the numerical method seems to be in agreement with the analytical ones and are independent of the mesh size for $n > 12$. The chern number calculation is most likely incorrect. Since it was only made using the results obtained from the purely numerical method, it is inconclusive.Concerning the analytical method, it enables one to see very clearly the marking features of the graphene DOS, such as the Dirac cone and the gap opening due to the next-nearest neighbour coupling. This result could be exploited to calculate other properties, such as the effective mass of the electrons and speed of phonons in the lattice.

REFERENCES

[1] D.S.L. Abergel et al. "Properties of graphene: a theoretical perspective". In: *Advances in Physics* 59.4 (2010), pp. 261–482. DOI: 10.1080/00018732.2010.487978. eprint: https://doi.org/10.1080/00018732.2010.487978. URL: https://doi.org/10.1080/00018732.2010.487978.

[2] János K Asbóth, László Oroszlány, and András Pályi. *A short course on topological insulators: Band structure and edge states in one and two dimensions*. Vol. 919. Springer, 2016.

[3] Yasuhiro; Suzuki Hiroshi Fukui Takahiro; Hatsugai. "Chern Numbers in Discretized Brillouin Zone: Efficient Method of Computing (Spin) Hall Conductances". In: *Journal of the Physical Society of Japan* 74 (6 June 2005). DOI: 10.1143/JPSJ.74.1674.

[4] "Graphene Flagship Annual Report 2016". In: (2016).

[5] F. D. M. Haldane. "Model for a Quantum Hall Effect without Landau Levels: Condensed-Matter Realization of the "Parity Anomaly"". In: *Phys. Rev. Lett.* 61 (18 1988), pp. 2015–2018. DOI: 10.1103/PhysRevLett.61.2015. URL: https://link.aps.org/doi/10.1103/PhysRevLett.61.2015.

[6] Takahiro; Aoki Hideo Hatsugai Yasuhiro; Fukui. "Topological analysis of the quantum Hall effect in graphene: Dirac-Fermi transition across van Hove singularities and edge versus bulk quantum numbers". In: *Physical Review B* 74 (20 Nov. 2006). DOI: 10.1103/PhysRevB.74.205414.

[7] A. K.; Morozov S. V.; Jiang D.; Katsnelson M. I.; Grigorieva I. V.; Dubonos S. V.; Firsov A. A. Novoselov K. S.; Geim. "Two-dimensional gas of massless Dirac fermions in graphene". In: *Nature* 438 (7065 2005). DOI: 10.1038/nature04233.

[8] K. S. Novoselov et al. "Electric Field Effect in Atomically Thin Carbon Films". In: *Science* 306.5696 (2004), pp. 666–669. ISSN: 0036-8075. DOI: 10.1126/science.1102896. eprint: http://science.sciencemag.org/content/306/5696/666.full.pdf. URL: http://science.sciencemag.org/content/306/5696/666.